Real-time Stability Analysis of Power Electronic Systems

Atle Rygg and Marta Molinas
Department of Engineering Cybernetics
Norwegian University of Science and Technology
Trondheim, Norway
Email: atle.rygg@ntnu.no

***Abstract*—The paper presents a new method for performing online stability analysis of power electronic systems. The method is based on impedance analysis, where the only information required are measurements taken at a single point. The proposed method injects current composed by several frequencies. The impedance is estimated at these frequencies, and the Vector Fitting method is used to estimate a continuous impedance model. The Nyquist Criterion is then applied to the fitted models of source and load subsystem impedance. The stability analysis is performed continuously with an update rate up to 10 Hz. The proposed method has been compared with the conventional frequency sweep method in an experimental setup.**

***Index Terms*—Impedance, Nyquist criterion, Power electronic systems, Real-time stability analysis.**

I. Introduction

Stability analysis of AC power systems with a high penetration of power electronics is important but difficult. The combination of multiple non-linearities and fast dynamics from controllers adds significant complexity to the analysis. Impedance-based analysis of AC power systems is a relevant and practical approach in this respect because it reduces the system into a source and load subsystem, and analyses the dynamic interactions between the two subsystem equivalents [1] [2]. The method is based on existing techniques for DC-systems, first applied in [3]. See Figure 1 for an overview of the principle. A general power system based on power electronic converters is partioned into a source and load subsystem. In the interface point a current source injects a disturbance. Current is injected in a way such that small-signal subsystem equivalents can be obtained from measurements of source current I_S, load current I_L as well as the voltage V. Based on these equivalents, a stability analysis can be performed based on the Generalized Nyquist Criterion (GNC) [4]. This criterion was first applied to AC systems in [2].

This method has some highly appealing properties. First, it considers the subsystems as "black-boxes", i.e. detailed knowledge of the parameters and properties of the system is not required as long as measurements can be obtained at its terminals. Furthermore, the impedance equivalents can be extracted based on measured signals in a real system. The most accurate method for this purpose is based on frequency sweeping [5]-[7]. However, frequency sweeping is not directly applicable in Real-time implementations since the duration for obtaining impedance equivalents can be up to several minutes.

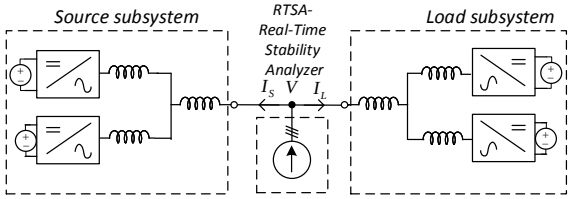

Fig. 1: Principal sketch of Real-time Stability Analyzer (RTSA) placed in a general power electronics based system.

The purpose of the paper is to bring the stability analysis as close to real time as possible.

Previous works have applied various methods to online estimate the source impedance. [8] provides a good overview of the classes of methods for this purpose. Furthermore, [8] proposes a method to obtain the momentary or instantaneous impedance, i.e. an impedance calculated multiple times within a fundamental frequency period. [9] and [10] estimated the source impedance seen from a converter by applying an impulse response. [11] carried out the same task by injecting a Discrete Interval Binary Sequence. [12] applies an Extended Kalman Filter for the grid impedance estimation where the resulting impedance equivalent is restricted to a first order RL-circuit. [13] present a stability analysis where measured grid impedance values are used in combination with calculated converter impedance values.

From the overview above it is concluded that most of the efforts on Real-time impedance measurements are focusing on the source impedance estimation only. The present work seeks to estimate both the source and load impedance simultaneously, in a similar way as the work based on frequency scanning [5]-[7]. The objective is to perform a stability analysis based on the Nyquist Criterion multiple times per second. An experimental setup called "Real Time Stability Analyzer" (RTSA) has been developed for this purpose, see Fig. 1. The paper is organized as follows: Impedance-based analysis for three-phase systems is described in section II. The experimental setup is presented in section III. The case study system and associated results are presented in section IV.

II. Impedance analysis of three-phase systems

Stability analysis by the impedance-based method was first introduced for DC-systems in [3]. The method is based on examining the ratio between source and load impedance as a function of frequency. Various stability criteria can be applied to this ratio, the most common is the Nyquist Criterion for DC-systems and the Generalized Nyquist Criterion (GNC) for three-phase systems [4].

A. Impedance models in different domains

In general, AC systems are more difficult to analyze than DC systems due to the fundamental frequency component. In other words, the system is never in true steady-state due to the alternating waveforms. Furthermore, three-phase systems are more challenging than single-phase systems due to the coupling between phases. The general structure of three-phase impedance models has matrix form:

$$\begin{bmatrix} V_a \\ V_a \\ V_c \end{bmatrix} = \begin{bmatrix} Z_{aa} & Z_{ab} & Z_{ac} \\ Z_{ba} & Z_{bb} & Z_{bc} \\ Z_{ca} & Z_{cb} & Z_{cc} \end{bmatrix} \begin{bmatrix} I_a \\ I_b \\ I_c \end{bmatrix} = \boldsymbol{Z_{abc}} \begin{bmatrix} I_a \\ I_b \\ I_c \end{bmatrix} \tag{1}$$

Note that all impedance elements are generally a function of the frequency. It is challenging to measure all nine elements in (1), therefore it is common to apply some kind of symmetry property. A widely adopted approach is to use the synchronous *dq* reference frame with following impedance model:

$$\begin{bmatrix} V_d \\ V_q \end{bmatrix} = \begin{bmatrix} Z_{dd} & Z_{dq} \\ Z_{qd} & Z_{qq} \end{bmatrix} \begin{bmatrix} I_d \\ I_q \end{bmatrix} = \boldsymbol{Z_{dq}} \begin{bmatrix} I_d \\ I_q \end{bmatrix} \tag{2}$$

Note that the zero sequence is disregarded from analysis, and hence the number of impedance elements is reduced into four. Impedance analysis in the *dq*-frame was first introduced in [2].

Another useful approach for impedance-based analysis is to apply symmetric components, also denoted the sequence domain. Again the zero sequence is disregarded, and the impedance model can be expressed as a 2x2 matrix based on the positive and negative sequence:

$$\begin{bmatrix} V_p \\ V_n \end{bmatrix} = \begin{bmatrix} Z_{pp} & Z_{pn} \\ Z_{np} & Z_{nn} \end{bmatrix} \begin{bmatrix} I_p \\ I_n \end{bmatrix} = \boldsymbol{Z_{pn}} \begin{bmatrix} I_p \\ I_n \end{bmatrix} \tag{3}$$

Impedance analysis in the sequence domain was first performed in [14]. Most works on sequence domain impedance analysis assumes zero cross-coupling between the positive and negative sequence, and hence the model can be rewritten as:

$$\begin{aligned} Z_p &= \frac{V_p}{I_p} \\ Z_n &= \frac{V_n}{I_n} \end{aligned} \tag{4}$$

Consequently, the 3x3 matrix in (1) has been simplified into two scalar equations without cross-coupling. Although some accuracy may be lost by these assumptions, the simplicity of (4) is highly appealing for practical purposes.

The relation between the *dq* impedance matrix (2) and the sequence domain impedance matrix (3) was derived in [15] on a general basis as:

$$\begin{aligned} \boldsymbol{Z_{pn}} &= A_Z \cdot \boldsymbol{Z_{dq}} \cdot A_Z^{-1} \\ \boldsymbol{Z_{dq}} &= A_Z^{-1} \cdot \boldsymbol{Z_{pn}} \cdot A_Z \\ A_Z = \frac{1}{\sqrt{2}} \begin{bmatrix} 1 & j \\ 1 & -j \end{bmatrix}, A_Z^{-1} &= A_Z^* = \frac{1}{\sqrt{2}} \begin{bmatrix} 1 & 1 \\ -j & j \end{bmatrix} \end{aligned} \tag{5}$$

An important note to these relations is that the positive and negative sequences are defined at two different frequencies, shifted with twice the fundamental. The coupling between these two frequencies was defined as the *Mirror Frequency Effect*. It was also shown in [15] that the necessary condition for (4) to be valid is that $Z_{dd} = Z_{qq}$ and $Z_{dq} = -Z_{qd}$.

The results presented in this paper is based on impedance analysis in the sequence domain. The coupling between positive and negative sequence has been neglected, i.e. no Mirror Frequency Effect is assumed. This assumption is made due to the challenge in online measurement of the off-diagonal elements.

B. Stability analysis by the Generalized Nyquist Criterion

As discussed in the introduction, the impedance-based stability analysis is conducted by means of the General Nyquist Criterion (GNC). The GNC is based on the minor-loop gain L of the system, which can be calculated as [2]:

$$L(s) = Z_S(s) \cdot Z_L(s)^{-1} \tag{6}$$

where $Z_S(s)$ is the *source subsystem impedance*, while $Z_L(s)$ is the *load subsystem impedance* (can be matrices or scalars). A common assumption in impedance-based analysis is to require a stable source when unloaded, and a stable load when connected to an ideal grid [1]. In this case the Generalized Nyquist Criterion states that the system is stable if and only if all roots of $L(s)$ do not encircle the point $(-1, 0)$ when drawn in the complex plane. Nyquist plots from the case study system based on (4) is presented in section IV.

C. Interpolating impedances by Vector Fitting

Vector Fitting (VF) is a well established method for rational approximation in the frequency domain using poles and residues [16] [17] [18]. The method is able to approximate a state-space model from a measured or computed transfer function. Vector Fitting is widely applied in many engineering fields, from high-voltage power systems to microwave systems and high-speed electronics. A Matlab-implementation of the method is available online [19].

In the context of impedance-based stability analysis, VF can be used to interpolate the impedance between the measured values. This is very useful when applying the Generalized Nyquist Criterion since this is a graphical method. In [20] a novel stability analysis method is proposed by using VF to extract the eigenvalues for the entire system based on measured impedance values.

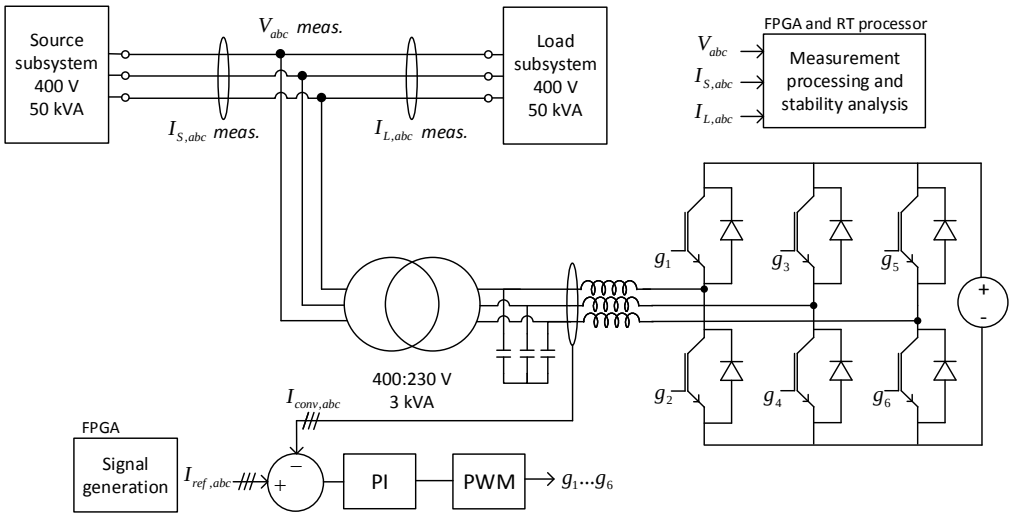

Fig. 2: Detailed schematic of RTSA power circuit

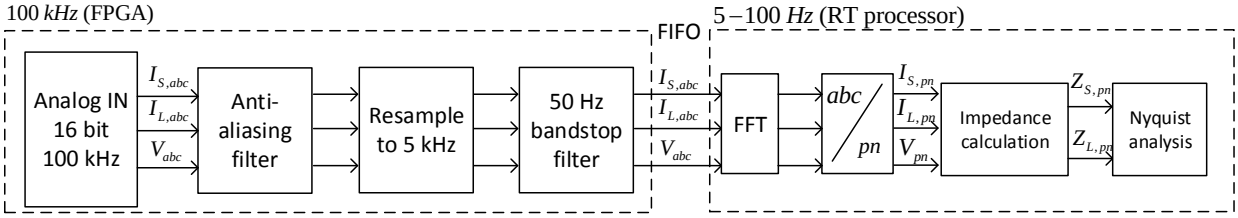

Fig. 3: Overview of measurement processing and signal generation

III. Measurement system overview

An overview of the Real-time Stability Analyzer (RTSA) placed in an example power electronics based system is presented in Figure 1. In principle it can be viewed as a three-phase current source connected in shunt at an arbitrary point in the system. The connection point determines the division of source and load subsystem.

A. Power circuit

The detailed schematic of the RTSA power circuit is shown in Figure 2. It is composed by the following elements:

- Three-phase Voltage Source Converter (VSC)
- LC-filter for switching harmonic attentuation
- Transformer (for galvanic insulation and filtering)
- DC-source
- Analog current PI-control (phase domain)

The switching frequency of the VSC is set to $f_{sw} = 20\ kHz$. This enables a current controller bandwidth in the range of *2 kHz*. The analog current controller takes as input the measured current $I_{conv,abc}$, as well as the three-phase reference current $I_{ref,abc}$. The reference is generated by an FPGA, and can be configured in different ways. Section III-C presents the two configurations applied in this work.

B. Measurements and processing

Three sets of three-phase measurements are required in the stability analysis: Source current $I_{S,abc}$, load current $I_{L,abc}$ and the voltage V_{abc}. All measurements are made by Hall effect sensors with appropriate ratings. A simplified flowchart of the data processing is presented in Figure 3. The fastest part of the data processing is performed on an FPGA. Each channel is simultaneously sampled at 100 kHz with 16 bit resolution. The data is then lowpass-filtered to avoid aliasing after resampling to 5 kHz. The fundamental frequency (50 Hz) components are then suppressed using a bandstop filter.

The resulting data are sent to a embedded processor through a First-in-First-out (FIFO) queue. The Fast Fourier Transform (FFT) is then performed, followed by a transformation from *abc*-domain to the sequence domain. The impedances are now estimated from the frequency domain sequence components (4). Only frequencies corresponding to the perturbation injection are considered. Details on the impedance estimation part is presented in section III-C. Finally, the Nyquist Criterion is used for stability analysis. The processor can be configured to perform the stability analysis at rates between 1-10 Hz. This choice depends on the applied injection frequencies.

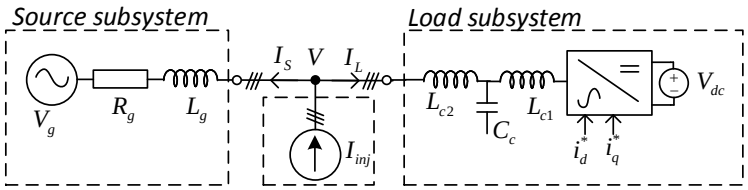

Fig. 4: Overview of three-phase case study system

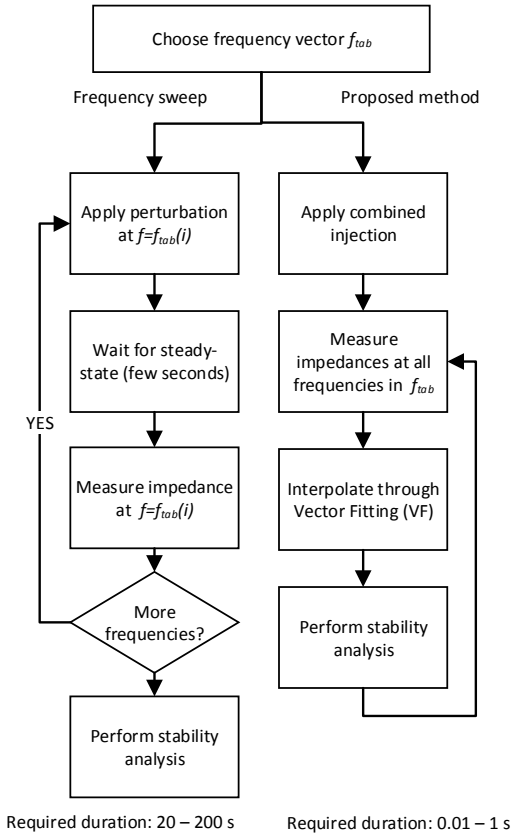

Fig. 5: Flowchart of frequency sweep and the proposed method

C. Perturbation injection strategy

When choosing injection strategy, there are three main objectives:

- Good accuracy
- Low injection amplitude
- Low time duration

These objectives are conflicting, leading to a set of trade-offs. Previous works discuss two main branches of methods. The first is called single-tone injection or frequency sweep, and is illustrated to the left in Fig. 5. In this method a sequence of frequencies are injected individually, and the response at the injection frequency is extracted. This is expected to be the most accurate method, and the required injection amplitude is low. The main drawback is the significant time required, which can be in the range of 20-200 seconds. Single-tone injection is therefore not a candidate for Real-time applications.

The other branch of methods is called wide-band or multi-tone injection. As the names suggest, the injection signal is composed by several frequencies, and it is therefore possible to estimate the impedance model from a single measurement. The duration depends on the injected frequencies, but can typically be in the range of 0.01-1 second. For Real-time stability analysis some kind of multi-tone injection is required, and a good trade-off between injection amplitude and accuracy must be sought.

The proposed method in this work is illustrated to the right in Fig. 5. An injection signal composed by several frequencies is continuously applied to the system. The number of frequencies lies typically in the range 5-10. The impedances at all injected frequencies can then be estimated by the processing algorithm in Fig. 3. The Vector Fitting method is then applied to interpolate the impedance values at frequencies between the injected ones, and the Nyquist stability analysis can be applied to the resulting impedance models. The operations in Fig. 5 can be performed in Real-time without problems, hence the Nyquist stability analysis can be performed at rates between 1 and 10 Hz, depending on the injection frequencies. A rate of 5 Hz has been applied for the results presented in this paper.

IV. Results

The experimental investigations in this paper are based on the system presented in Fig. 4. A Voltage Source Converter (VSC) is operated with *dq* current control and a constant DC-link voltage. It is equipped with an output LCL-filter, and is synchronized to the grid by a Phase-Lock-Loop (PLL). The grid is a 230 V three-phase supply interfaced with additional impedance R_g and Z_g. The RTSA is represented as a current source I_{inj}, and is connected in the interface point as seen in the figure.

TABLE I: Parameter values and operation point

Parameter	Value	Parameter	Value
Grid voltage V_g	230 V	Rated grid current	10 A
Converter DC-voltage V_{dc}	350 V	Filter inductance L_{c1}	500 μH
Filter inductance L_{c2}	200 μH	Filter capacitance C_c	50 μF
d-axis reference i_d^*	$5A$	q-axis reference i_q^*	5 A

Key parameter values and operation point are summarized in Table I. The following injection frequencies have been applied in the experiments:

$$f_{tab,pos} = \begin{bmatrix} 230 & 390 & 720 & 970 & 1340 & 1620 \end{bmatrix} Hz$$
$$f_{tab,neg} = \begin{bmatrix} 30 & 220 & 540 & 920 & 1340 & 1660 \end{bmatrix} Hz \quad (7)$$

Note that positive sequence frequencies below 230 Hz are avoided due to a challenge presented in section IV-C. The reference amplitude for every injection frequency is set to $I_{inj} = 0.2$ A.

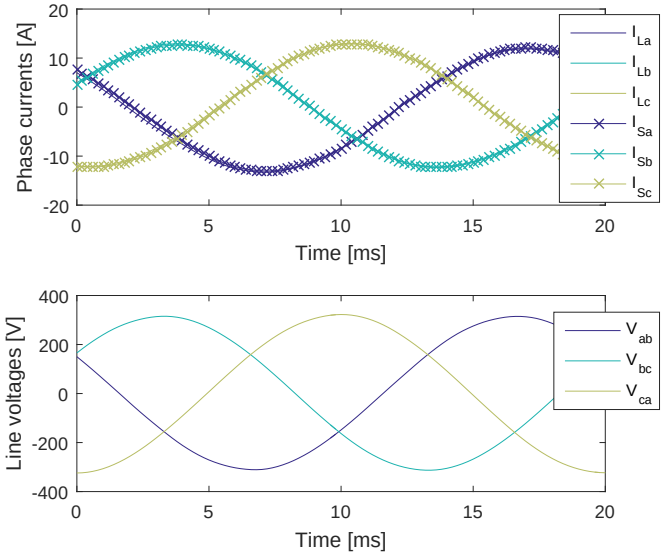

Fig. 6: Voltage and current measurements *without injection*

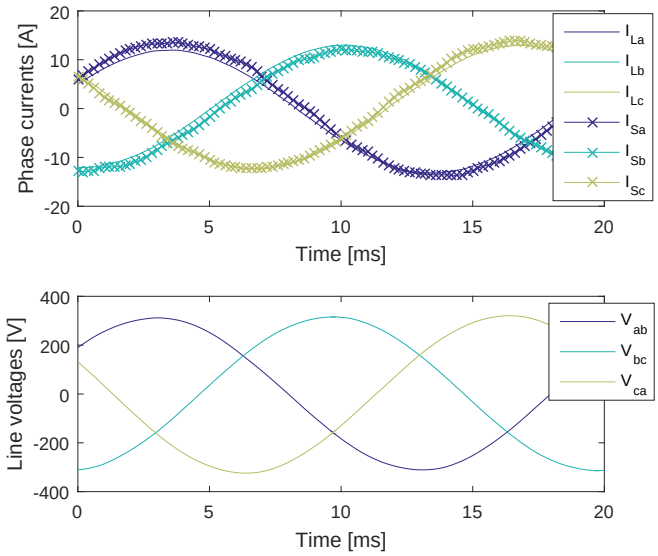

Fig. 7: Voltages and current measurements *with injection*

A. Time-domain measurements

To illustrate how the system current and voltages are affected by this injection, measurements with and without injection are presented in Fig. 6 and Fig. 7. The measurements *without* injection show balanced sets of three-phase voltages and currents. The load current I_L equals the source current I_S as expected since there is no injection.

When injection is added, the current waveforms are slightly distorted. The source current is more distorted, and this is expected since $|Z_S| < |Z_L|$ for most frequencies. Consequently, most of the injected current will flow towards the grid. The voltage waveforms appear close to unaffected by the injection. This is explained by a combination of low injected current amplitude and low impedance values. The induced voltages at the injection frequencies are in the range of 1 V, which is less than a percent of the fundamental value.

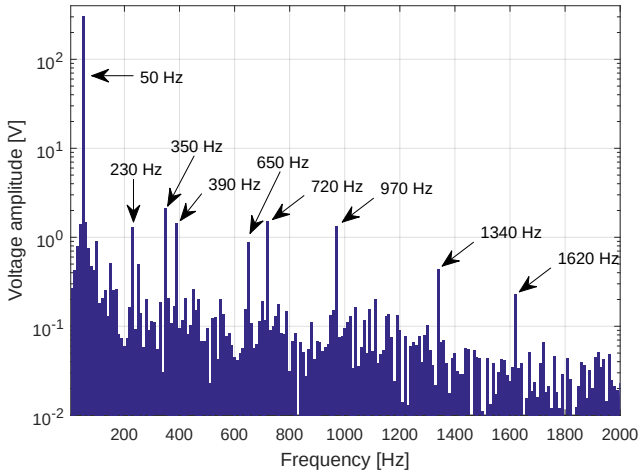

Fig. 8: Positive sequence voltage spectrum without (upper) and with (lower) 50 Hz bandstop filter

B. Frequency domain example

A snapshot of the positive sequence voltage FFT is presented in Fig. 8. The window length is 100 ms., leading to a 10 Hz resolution in the frequency domain. The fundamental frequency component is dominating, which was also the conclusion from Fig 7. The low-order positive sequence integer harmonics are present: 5^{th} and 11^{th}. The injection frequencies are all visible in the FFT plot, and hence it is possible to estimate the impedances at these frequencies.

One major challenge is identified from the FFT plots. Although the fundamental frequency is very close to 50 Hz, even the slightest deviation will introduce spectral leakage. Since the magnitude of the fundamental is more than 100 times larger than the injection frequencies, the spectral leakage can lie in the range of the injection magnitudes. The spectral leakage will add an artificial component to the injection frequencies, and this will corrupt impedance calculation. From the FFT snapshot in Fig. 8 it is observed that the ratio between injection magnitude and the nearby spectral leakage level is between 5 and 10. To overcome this problem, the fundamental frequency bandstop filter is included in the signal processing (Fig. 3).

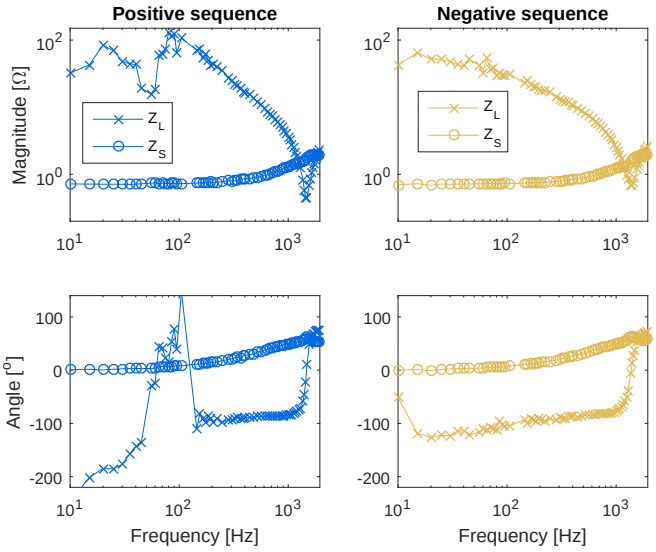

Fig. 9: Results from experimental frequency sweep

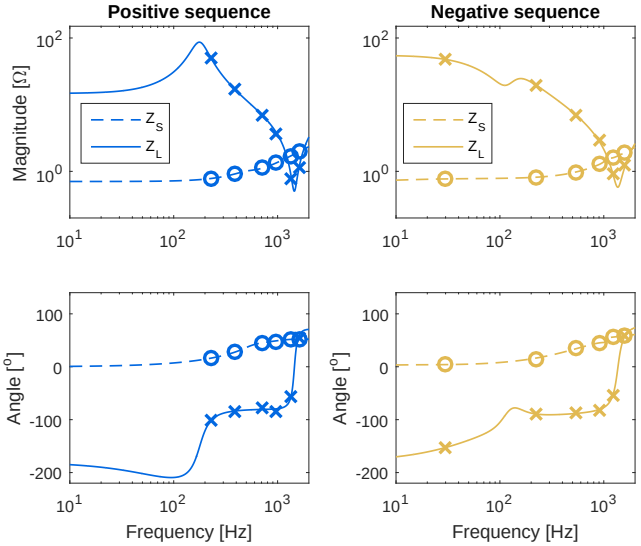

Fig. 10: Impedance measurements by the proposed method. 'x' represents measured values, lines are the vector fit.

C. Impedance analysis

The positive and negative sequence impedances (4) have been calculated based on the two methodologies in Fig. 5. The coupling between positive and negative sequence has been neglected as discussed in section II-A. The resulting measurement from the frequency sweep method is presented in Fig. 9. The source impedance Z_S has a typical RL-characteristic as expected, and this is similar for both sequences. The resistance is dominating up to approximately 200 Hz.

The load impedance Z_L has a capacitive behavior at frequencies below 1500 Hz. After this frequency the impedance appears inductive. The series resonance at 1500 Hz can be explained by the converter LCL-filter. This pattern is similar for both sequences. The positive sequence impedance has a strongly non-linear trajectory in the range 20-100 Hz. A possible explanation to this is that the system is not MFD at these frequencies. At frequencies in the vicinity of the fundamental, the PLL will cause a coupling between the so-called mirror frequencies [15]. This effect can only be accurately captured by a 2x2 matrix impedance representation as in (2) or (3). Further work will extend the proposed methodology to also account for mirror frequency coupling.

The impedance trajectories by the proposed method is presented in Fig. 10. The injected frequencies for positive and negative sequence are given in (7). The impedance measurements are represented by 'x' and 'o'. The Vector Fitting method is then used to obtain a continuous impedance model, represented by lines. It is clear that the fitted curve match well with the result from the frequency sweep. The series resonance is captured accurately, and also the behaviour at lower frequencies is well estimated. The main exception is the non-linear behaviour for positive sequence load impedance around the fundamental (50 Hz). As this behaviour is assumed to be caused by violation of the MFD-assumption, it is very hard to capture with any curve fitting technique.

D. Nyquist stability analysis

The purpose of establishing impedance equivalents in the previous section is to apply an online Nyquist criterion analysis. This analysis is straightforward once the impedance curves are established. The ratio $L(s)$ between source and load impedance has been calculated separately for the source and load impedance (6). This has been performed both for the frequency sweep impedances (Fig. 9) and for the proposed method (Fig. 10). The results are presented in Fig. 11, where "RT" denotes the proposed method (Real-time), and "sweep"

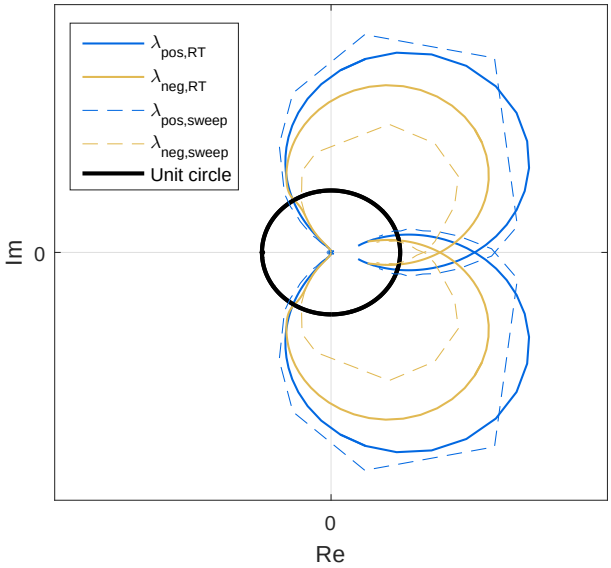

Fig. 11: Nyquist plot based on Fig. 9 and 10 'RT'=proposed method, 'sweep'=frequency sweep.

denotes frequency sweep. The unity circle is represented as the black solid line.

The match between the Nyquist curves of the frequency sweep and the proposed method is generally good. The proposed method has very smooth Nyquist curves due to the vector fitting interpolation, while the frequency sweep is composed by line segments between the measured values. For positive sequence the curves close to overlap, while there is a slight deviation in the negative sequence amplitude.

V. Conclusion and further work

This paper has presented a new method for Real-time stability analysis of power electronic systems. The method is based on simultaneous current injection of a low number of frequencies. The vector fitting method is applied to establish a continuous impedance model, and the Nyquist Criterion is applied to these impedance models. The accuracy of the method has been verified through a comparison with the conventional frequency sweep method. While the frequency sweep method is considered to be more accurate, the proposed method requires less than one second to update the Nyquist plot. The frequency sweep requires several minutes.

A number of improvments is suggested as further work. First is to extend the method to also take into account the coupling between positive and negative sequence. This is required for accurate stability analysis at frequencies where mirror frequency coupling exist. Another improvement is to subsitute FFT with another method for impedance estimation. The FFT is associated with relatively poor signal-to-noise ratio and spectral leakage issues. Finally, improved methods for disturbance injection should be considered in order to reduce the injection amplitude to a minimum. This is important if such method shall be implemented in actual systems. Otherwise the injection can lead to power quality issues.

References

[1] J. Sun, "Small-signal methods for ac distributed power systems;a review," *Power Electronics, IEEE Transactions on*, vol. 24, no. 11, pp. 2545–2554, Nov 2009.

[2] M. Belkhayat, *Stability criteria for AC power systems with regulated loads*. Purdue University, 1997.

[3] R. D. Middlebrook, "Input filter considerations in design and application of switching regulators," in *IEEE Industry Applications Society Annual Meeting*, 1976.

[4] C. Desoer and Y.-T. Wang, "On the generalized nyquist stability criterion," *Automatic Control, IEEE Transactions on*, vol. 25, no. 2, pp. 187–196, Apr 1980.

[5] G. Francis, R. Burgos, D. Boroyevich, F. Wang, and K. Karimi, "An algorithm and implementation system for measuring impedance in the d-q domain," in *Energy Conversion Congress and Exposition (ECCE), 2011 IEEE*, Sept 2011, pp. 3221–3228.

[6] Y. Familiant, J. Huang, K. Corzine, and M. Belkhayat, "New techniques for measuring impedance characteristics of three-phase ac power systems," *Power Electronics, IEEE Transactions on*, vol. 24, no. 7, pp. 1802–1810, July 2009.

[7] J. Huang, K. Corzine, and M. Belkhayat, "Small-signal impedance measurement of power-electronics-based ac power systems using line-to-line current injection," *Power Electronics, IEEE Transactions on*, vol. 24, no. 2, pp. 445–455, Feb 2009.

[8] R. Stiegler, J. Meyer, P. Schegner, and D. Chakravorty, "Measurement of network harmonic impedance in presence of electronic equipment," in *Applied Measurements for Power Systems (AMPS), 2015 IEEE International Workshop on*. IEEE, 2015, pp. 49–54.

[9] Z. Staroszczyk, "A method for real-time, wide-band identification of the source impedance in power systems," *Instrumentation and Measurement, IEEE Transactions on*, vol. 54, no. 1, pp. 377–385, 2005.

[10] M. Cespedes and J. Sun, "Online grid impedance identification for adaptive control of grid-connected inverters," in *Energy Conversion Congress and Exposition (ECCE), 2012 IEEE*, Sept 2012, pp. 914–921.

[11] T. Roinila, M. Vilkko, and J. Sun, "Online grid impedance measurement using discrete-interval binary sequence injection," *Emerging and Selected Topics in Power Electronics, IEEE Journal of*, vol. 2, no. 4, pp. 985–993, Dec 2014.

[12] N. Hoffmann and F. Fuchs, "Minimal invasive equivalent grid impedance estimation in inductive-resistive power networks using extended kalman filter," *Power Electronics, IEEE Transactions on*, vol. 29, no. 2, pp. 631–641, Feb 2014.

[13] L. Jessen and F. W. Fuchs, "Modeling of inverter output impedance for stability analysis in combination with measured grid impedances," in *Power Electronics for Distributed Generation Systems (PEDG), 2015 IEEE 6th International Symposium on*. IEEE, 2015, pp. 1–7.

[14] J. Sun, "Impedance-based stability criterion for grid-connected inverters," *Power Electronics, IEEE Transactions on*, vol. 26, no. 11, pp. 3075–3078, Nov 2011.

[15] A. Rygg, M. Molinas, Z. Chen, and X. Cai, "A modified sequence domain impedance definition and its equivalence to the dq-domain impedance definition for the stability analysis of ac power electronic systems," *Submitted to IEEE Journal of Emerging and Selected Topics in Power Electronics (in second review)*, 2016.

[16] B. Gustavsen and A. Semlyen, "Rational approximation of frequency domain responses by vector fitting," *Power Delivery, IEEE Transactions on*, vol. 14, no. 3, pp. 1052–1061, Jul 1999.

[17] B. Gustavsen, "Improving the pole relocating properties of vector fitting," *Power Delivery, IEEE Transactions on*, vol. 21, no. 3, pp. 1587–1592, July 2006.

[18] D. Deschrijver, M. Mrozowski, T. Dhaene, and D. De Zutter, "Macromodeling of multiport systems using a fast implementation of the vector fitting method," *Microwave and Wireless Components Letters, IEEE*, vol. 18, no. 6, pp. 383–385, June 2008.

[19] "The vector fitting web page," https://www.sintef.no/projectweb/vectfit/.

[20] A. Rygg, M. Amin, M. Molinas, and B. Gustavsen, "Apparent impedance analysis - a new method for power system stability analysis," in *Seventeenth IEEE Workshop on Control and Modeling for Power Electronics, COMPEL*, 2016.